arXiv:hep-ph/9905412v1 20 May 1999

NLL Corrections for B-Meson Radiative Exclusive Decays

H. H. Asatryan[a], H. M. Asatrian[a], D. Wyler[b]

[a]Yerevan Physics Institute, Alikhanyan Br., 375036-Yerevan, Armenia
[b] Institute for Theoretical Physics, University of Zürich, Zürich, Switzerland

Abstract

We calculate the next-to-leading corrections to the branching ratio of exclusive $B \to K^*\gamma$ decay. The renormalization scale dependence is reduced compared to the leading logarithmic result but there remains a dependence on a cutoff parameter of the hadronic model. The calculated corrections increase the predicted branching ratio by about 10%, but it remains in agreement with the experimental value.

1 Introduction

The rare neutral flavor changing decays of B-meson are generally considered a good testing ground for new physics [1]. The inclusive decay $b \to s\gamma$ has therefore received intensive experimental [2] and theoretical attention [3]-[11]. In particular, the next-to-leading order calculation for the standard model strongly improved the theoretical uncertainties, most notably the scale dependence of the perturbative calculation.

The calculation of the decay rates for the corresponding exclusive decays such as $B \to K^*\gamma$ [12] is usually much more complex because of bound state effects (for a recent work, see for instance [13]). But they are easier to observe, and so it is also of interest to calculate their branching ratios and direct CP asymmetries to the highest possible precision. In this paper we consider the branching ratio for $B \to K^*\gamma$ in the next-to-leading logarithmic approximation. The decay $B \to \rho\gamma$ can in principle be treated in the same way, but there are several additional contributions which require new methods.

In [14], the $B \to \rho\gamma$ and $B \to K^*\gamma$ branching ratios and rate asymmetries were investigated in the leading logarithmic approximation within a simple meson model. Although this model does not give completely correct results (in particular the ratio of the semileptonic π and ρ decays), we will also use it in this work, because of its simplicity.

As usual, the basis of the calculation is the effective Hamiltonian which we record here for completeness. For $B \to K^*\gamma$ decay it has the form [14]

$$\mathcal{H}_{eff} = -\frac{4G_F}{\sqrt{2}}\left\{\Sigma_i v_t C_i(\mu) O_i(\mu) - v_u\left[C_1(\mu)(O_{1u}(\mu) - O_1(\mu)) + C_2(\mu)(O_{2u}(\mu) - O_2(\mu))\right]\right\}, \tag{1}$$

where $v_a = V_{tb}V^*_{as}$, a=u,c,t, i=1,2,...8. For the decay $B \to \rho\gamma$ one must replace v_a by $v^{'}_a$, with $v^{'}_a = V_{tb}V^*_{ad}$. The operators O_i can be found in many places [8, 15, 16].

2 The bound state model

As mentioned, we will use a simple model for the mesons to take into account the bound state effects [14, 17] (for other approaches, see [18],[19]). The B and the K^* are described by two constituents: $B = (b, \bar{q})$, $K^* = (s, \bar{q})$. The sum of the four momenta of the constituents equals that of the bound state. The mass of the spectator antiquarks is taken to be zero and the b-quark mass becomes momentum dependent:

$$m_b = \sqrt{m_B^2 - 2p_B p_q}, \tag{2}$$

where p_B and p_q are the four momenta of the B-meson and spectator quark, respectively. The momentum p_q in the B-meson rest frame is restricted to

$$|p_q| = E < m_B/2. \tag{3}$$

The B meson is represented by a matrix Ψ_B

$$\Psi_B = C_B \int \frac{d^3p_q}{2E_q(2\pi)^3}\sqrt{\frac{m_B}{2(m_B^2 - p_B p_q)}}\,\phi_B(|p_B p_q|/m_B)\Sigma_b \times \frac{1}{\sqrt{N}}1_N$$

$$\Sigma_B = -(\hat{p}_b + m_b)\gamma_5\hat{p}_q, \qquad \phi_B(p) = \exp(-p^2/(2p_F^2)), \tag{4}$$

where C_B is a normalization factor and p_F is fixed in such a way that one obtains the correct value of B-meson decay constant f_B. The 'hat' symbol stands for the usual 'slash'.

The final state vector meson K^* is represented by two constituents with parallel momenta $p_s = yp_V$, $p_q = (1-y)p_V$. In most cases its mass and that of the constituent s quark can be neglected (see however the discussion of that point in section 4). It is described by the matrix

$$\begin{aligned} \Psi_V &= C_V \int_0^1 dy \phi_V(y) \Sigma_V \times \frac{1}{\sqrt{N}} 1_N, \qquad C_V = f_V/(4\sqrt{N}) \\ \Sigma_V &= \lim_{m_V \to 0} \hat{\epsilon}_V^* (\hat{p}_V + m_V), \qquad \phi_V(y) = 6y(1-y)(1+\cdots), \end{aligned} \tag{5}$$

where $\phi_V(y)$ for $V = K^*, \rho$ are given by [19, 20]:

$$\begin{aligned} \phi_{K^*}(y) &= 6y(1-y)(1 + 0.57(2y-1) - 1.35((2y-1)^2 - 1/5) + \\ &+ 0.46(7(2y-1)^3/3 - (2y-1))) \\ \phi_\rho(y) &= 6y(1-y)(1 - 0.85((2y-1)^2 - 1/5)). \end{aligned} \tag{6}$$

The $B \to K^*\gamma$ transition matrix elements have a following general form:

$$< V\gamma|O_i|B >= e m_B \epsilon_\gamma^\mu \left[i\epsilon_{\mu\nu\alpha\beta} p_\gamma^\nu \epsilon_V^\alpha p_V^\beta F_1[O_i] + ((p_\gamma \epsilon_V) p_{V\mu} - (p_\gamma p_V) \epsilon_{V\mu}) F_5[O_i] \right]. \tag{7}$$

For a massless final state meson we have $F_1 = F_5$.

In our model, the hadronic matrix elements are written as

$$\begin{aligned} < V\gamma|O_i|B > &= C_B C_V \int \frac{d^3 p_q dy}{(2\pi)^3 2E_q} \sqrt{\frac{m_B}{2(m_B^2 - p_B p_q)}} \\ &\times \phi_B\left(\frac{p_B p_q}{m_B}\right) \phi_V(y) \frac{1}{N} Tr\left[\Sigma_V M_{sb} \Sigma_B M_{qq'}\right], \end{aligned} \tag{8}$$

where the trace is in Dirac and color space and the matrices M_{sb} and $M_{qq'}$ are related to the quark-level matrix elements by

$$< s\bar{q}^{'}\gamma|O_i|b\bar{q} >= \bar{u}_s M_{sb} u_b \bar{v}_q M_{qq'} v_{q'}. \tag{9}$$

The decay width in NLL approximation can be written as

$$\Gamma(B \to V\gamma) = |v_t|^2 G_F^2 \alpha_{em} m_B^5 \sum_l |\sum_i C_i F_l[O_i]|^2 \left(1 - \frac{8}{3}\frac{\alpha_s}{\pi}\right). \tag{10}$$

In leading approximation only O_7 contributes and the last parenthesis is simply one.

In order to eliminate some of the uncertainties of the model, we write

$$BR(B \to V\gamma) \equiv \frac{\Gamma(B \to V\gamma)}{\Gamma_{sl}} BR(B \to Xl\nu_l), \tag{11}$$

where Γ_{sl} in NLL approximation is given by

$$\begin{aligned} \Gamma_{sl} &= \frac{G_F^2}{192\pi^3} |V_{cb}|^2 C_B^2 \int \frac{d^3 p_q}{(2\pi^3)} |\phi_B(|p_q|)|^2 \frac{m_b^6}{m_B - E_q} g(r) \left(1 - \frac{2\alpha_s}{3\pi} f(r)\right) \\ g(r) &= 1 - 8r^2 + 8r^6 - r^8 - 24r\log(r) \\ f(r) &= (\pi^2 - \frac{31}{4})(1-r)^2 + \frac{3}{2}, \qquad r = m_c/m_b(p_q) \end{aligned} \tag{12}$$

and we use the experimental value for the semileptonic decay, $BR(B \to Xl\nu_l)$=0.103 [21].

3 The “inclusive amplitudes”

Consider first the decay graphs where the spectator is not touched; they are very similar to the inclusive decays. As mentioned, in leading logarithmic approximation only $F[O_7]$ contributes to $< V\gamma|\mathcal{H}|B >$ (Fig. 1). Evaluating the trace, one gets [14]:

$$F^0[O_7] = -\frac{\sqrt{m_B}C_B C_V}{4\pi^2} \int dy \frac{y}{\sqrt{1+y}} \phi_V(y) \phi_B \left(\frac{m_B(1-y))}{2} \right). \tag{13}$$

Here, and everywhere we will set $F_1 = F_5 \equiv F$ for all form factors. The deviation due to small final state masses can be neglected.

For the NLL amplitudes, we can use the results for NLL inclusive O_7, O_2, O_2 amplitudes given in [8]

$$\begin{aligned}
&< s\gamma|O_7|b > = < s\gamma|O_7|b >_{tree} \left(1 + \frac{\alpha_s(m_b)}{4\pi} \left(\gamma_{77}^{(0)eff} \log(m_b/\mu) + r_7\right)\right) \\
&< s\gamma|O_2|b > = < s\gamma|O_7|b >_{tree} \frac{\alpha_s(m_b)}{4\pi}(l_2 \log(m_b/\mu) + r_2) \\
&< s\gamma|O_8|b > = < s\gamma|O_7|b >_{tree} \frac{\alpha_s(m_b)}{4\pi}(l_8 \log(m_b/\mu) + r_8) \\
&< s\gamma|O_7|b >_{tree} = m_b \frac{e}{8\pi^2} \bar{u}(p^{'}) \hat{\epsilon} \hat{q} u(p),
\end{aligned} \tag{14}$$

where the expressions for r_2, r_7, r_8, l_2, $\gamma_{77}^{(0)eff}$, l_8 are given in [8].

The problem of Bremsstrahlung corrections needs discussion. In the inclusive case the infrared divergences from the NLL calculation (loops) of $< s\gamma|O_7|b >$ (Fig. 2) cancels at the level of the decay width when one adds Bremsstrahlung corrections associated with the operator O_7 (that is when we sum over final states with additional soft gluons). In the exclusive case the situation is much more complicated. Normally we consider the mesons to contain only two constituents (quark and antiquark) in a color singlet state. Therefore, it is not possible to simply add to the Hilbert space of hadrons states with extra gluons; furthermore, soft gluons are not physical. Instead, these gluons must be incorporated into the physical hadrons, making it necessary to consider three particle states (quark, antiquark and gluon) etc for the K^* meson and other physical particles. For a discussion of this point see [22].

This well known problem cannot be really solved with the present methods and one must resort to approximate methods (Additional IR problems connected to the exchange of gluons with the spectator quark will be discussed shortly).

We have therefore used two heuristic methods to obtain finite results. In Method 1 we use the fact that we could write the finite 'total inclusive amplitude' (including the bremsstrahlungsgluon) as an effective matrix element for $b \to s\gamma$ as in equation (3.5) of [8]. There, this was just a mathematical trick to obtain a convenient form of the result up to the desired accuracy. Physically, we might envisage it as a replacement of the eight gluons by an abelian vector. This interpretation follows if one calculates the cross section of the bremsstrahlungsprocess which consists in summing over the final states and where the sum over the gluons indeed yields an 'abelian' contribution (with the correct factor). In this way the final result is simply

$$\begin{aligned}
F^{incl}[O_7] = & - \frac{C_B C_V \sqrt{m_B}}{4\pi^2} \frac{\alpha_s(m_b)}{4\pi} (\gamma_{77}^{(0)eff} \log(m_b/\mu) + r_7) \times \\
& \times \int dy \frac{y}{\sqrt{(1+y)}} \phi_V(y) \phi_B \left(\frac{m_B(1-y)}{2} \right) \\
F^{incl}[O_8] = & - \frac{C_B C_V \sqrt{m_B}}{4\pi^2} \frac{\alpha_s(m_b)}{4\pi} (l_8 \log(m_b/\mu) + r_8) \times \\
& \times \int dy \frac{y}{\sqrt{(1+y)}} \phi_V(y) \phi_B \left(\frac{m_B(1-y)}{2} \right) \qquad (15) \\
F^{incl}[O_2] = & - \frac{C_B C_V \sqrt{m_B}}{4\pi^2} \frac{\alpha_s(m_b)}{4\pi} (l_2 \log(m_b/\mu) + r_2) \times \\
& \times \int dy \frac{y}{\sqrt{(1+y)}} \phi_V(y) \phi_B \left(\frac{m_B(1-y)}{2} \right).
\end{aligned}$$

In (3) and (4) r_8 and r_2 include real and imaginary part [8].

In Method 2 we cut the virtual loop momenta at a value Λ. The same cutoff Λ is then used for the momentum when calculating the O_7 diagram (Fig. 3 a,b) with a gluon exchanged between the quark lines (next section). No Bremsstrahlung corrections are then added. The physical picture here is that gluons with momenta below Λ are embodied in the hadronic wave function. The formulae for the contribution of the operator O_7 with a cutoff are given in Appendix A.

4 NLL "exclusive" amplitudes

Next consider the 'exclusive' amplitudes, i.e. amplitudes which include the exchange of gluon between two quark lines.
As mentioned above, we require the gluons to be of-shell by at least an amount Λ^2. In the numerical evaluation, we will consider the three cases Λ =0.2,0.5,1GeV.

4.1 Contributions from O_2

The form factors associated with O_2 originate from two types of diagrams (Fig. 4a, b). When the photon is emitted from external quark lines (Fig. 4a), we can use the expression for the effective $b\bar{s}g$ vertex given in [8, 14]

$$I_\mu^a = \frac{g_s}{16\pi^2} \left(q^2 \gamma_\mu - q_\mu \hat{q} \right) L \frac{\lambda^a}{2} V \left(\frac{q^2}{m_i^2} \right) \qquad (16)$$

$$V\left(\frac{q^2}{m_i^2}\right)=4\Gamma(\epsilon)\mu^{2\epsilon}\exp(\gamma_E\epsilon)(1-\epsilon)\exp(i\pi\epsilon)\int_0^1 dx[x(1-x)]^{1-\epsilon}\left[q^2-\frac{m_i^2}{x(1-x)}+i\delta\right]^{-\epsilon}.$$

The explicit calculation of V(r) ($r=\frac{q^2}{m_i^2}$) gives:

$$V(r)=\frac{2}{3}\frac{1}{\epsilon}+\frac{2}{3}\log\frac{\mu^2}{m_i^2}+\frac{4}{9}\frac{6+r}{r}+\frac{4}{3}\frac{(r^2-2r-8)}{r\sqrt{r(4-r)}}\arctan\sqrt{\frac{r}{4-r}} \tag{17}$$

for $r<4$, and

$$V(r)=\frac{2}{3}\frac{1}{\epsilon}+\frac{2}{3}\log\frac{\mu^2}{m_i^2}+\frac{4}{9}\frac{6+r}{r}+\frac{2}{3}\frac{(r^2-2r-8)}{r\sqrt{r(4-r)}}\log\frac{\sqrt{r}-\sqrt{r-4}}{\sqrt{r}+\sqrt{r-4}}+$$
$$+\frac{2}{3}i\frac{r+2}{r}\sqrt{\frac{r-4}{r}} \tag{18}$$

for $r>4$. We see that $V(r)$ contains an infinity $\frac{1}{\epsilon}$, where ϵ is the parameter which comes from the dimensional regularization method used. It is of course cancelled by an appropriate counter-term. The contribution from $V(r)$ to the effective Hamiltonian then has the following form

$$C_2V(r)\frac{\alpha_s}{4\pi}\frac{1}{q^2}\left(\bar{s}\frac{1}{2}\lambda^a(\gamma_\mu q^2-q_\mu\hat{q})Lb\right)\left(\bar{u}\gamma_\mu\frac{1}{2}\lambda^a u\right), \tag{19}$$

while that of the counter-term reads:

$$\begin{aligned}&-\frac{4}{3}C_2\frac{\alpha_s}{48\pi\epsilon}<s\bar{u}\gamma|O_3|b\bar{u}>+3\frac{4}{3}C_2\frac{\alpha_s}{48\pi\epsilon}<s\bar{u}\gamma|O_4|b\bar{u}>-\\&-\frac{4}{3}C_2\frac{\alpha_s}{48\pi\epsilon}<s\bar{u}\gamma|O_5|b\bar{u}>+3\frac{4}{3}C_2\frac{\alpha_s}{48\pi\epsilon}<s\bar{u}\gamma|O_6|b\bar{u}>.\end{aligned} \tag{20}$$

It is easy to see the cancellation of the divergences proportional to $\frac{1}{\epsilon}$ using the formula $\sum_r\frac{1}{2}\lambda^r_{ab}\frac{1}{2}\lambda^r_{cd}=\frac{1}{6}(3\delta_{ad}\delta_{bc}-\delta_{ab}\delta_{cd})$.
Summing over all diagrams where the photon is emitted from different external quark lines we finally obtain for the form-factor in the rest frame of the B-meson

$$\begin{aligned}F^1[O_2]&=\frac{g_s^2}{16\pi^2}\frac{N^2-1}{2N}\frac{1}{m_B^2}\int\phi_B(E_q)\phi_V(y)\frac{1}{\sqrt{2(m_B-E_q)}}\frac{E_q^2}{\pi^2}dE_qdzdy\times\\&\times\left(-Q_d\frac{V(r_1)}{y}+Q_u\frac{V(r_2)}{1-y}\right),\end{aligned} \tag{21}$$

where $Q_u=2/3$, $Q_d=-1/3$, $r_1=((1-y)p_V-p_q)^2$, $r_2=((1-y)p_V+p_\gamma-p_q)^2$, $z=\cos\theta$ and θ is the angle between the spectator quarks in the B and K^*-mesons, respectively.
When the photon is emitted from the quarks in the internal loop (Fig 4b), we will use the following expression for the effective $\bar{s}bg\gamma$-vertex [14]:

$$\begin{aligned}I^a_{\mu\nu}=-\frac{g_seQ_u}{8\pi^2}\frac{\lambda^a}{2}\Big[&i\epsilon_{\beta\mu\nu\alpha}(q^\beta\Delta i_5+p_\gamma^\beta\Delta i_6)+\\&+i\frac{\epsilon_{\rho\sigma\mu\alpha}}{p_\gamma\cdot q}q^\rho p_\gamma^\sigma q_\nu\Delta i_{23}+i\frac{\epsilon_{\rho\sigma\nu\alpha}}{p_\gamma\cdot q}q^\rho p_\gamma^\sigma p_{\gamma\mu}\Delta i_{26}\Big]\gamma^\alpha L,\end{aligned} \tag{22}$$

where q is the momentum of the gluon. The quantities $\Delta i_n = \Delta i_n(z_0, z_1, z_2)$ are functions of the variables $z_0 = s/m_i^2, z_1 = q^2/m_i^2, z_2 = p_\gamma^2/m_i^2$, and s is the invariant mass of the internal quark pair. When the photon is on-shell we have

$$\begin{aligned}\Delta i_5(z_0, z_1, 0) &= -1 + \frac{z_1}{z_0 - z_1}\left(Q_0(z_0) - Q_0(z_1)\right) - \frac{2}{z_0 - z_1}\left(Q_-(z_0) - Q_-(z_1)\right) \\ \Delta i_6(z_0, z_1, 0) &= 1 + \frac{z_1}{z_0 - z_1}\left(Q_0(z_0) - Q_0(z_1)\right) + \frac{2}{z_0 - z_1}\left(Q_-(z_0) - Q_-(z_1)\right) \\ \Delta i_{23}(z_0, z_1, 0) &= \Delta i_5(z_0, z_1, 0) = -\Delta i_{26}(z_0, z_1, 0).\end{aligned} \tag{23}$$

The functions Q_0 and Q_- are defined in the following way:

$$Q_-(x) = -2\pi i \log\left(\frac{\sqrt{x} + \sqrt{x-4}}{2}\right) - x\int_0^1 du \frac{(2u-1)\log u}{1 - xu(1-u)} \tag{24}$$

$$Q_0(x) = -\pi i \sqrt{\frac{x-4}{x}} - x\int_0^1 du \frac{u(2u-1)}{1 - xu(1-u)}. \tag{25}$$

The expression for the form factor is the following:

$$F^2[O_2] = \alpha_s C_B C_V C_N \int \phi_B(E_q)\phi_V(y) \frac{Q_u e^2}{\sqrt{2(m_B - E_q)}} \frac{E_q^2}{16 q^2 \pi^3} dE_q dz dy \times \tag{26}$$

$$\times\left(\frac{4(1-z)E_q}{m_B}\Delta_{i_5} - 4\Delta_{i_6} + 2\frac{(1-z^2)E_q^2}{p_\gamma \cdot q}\Delta_{i_{23}} + \frac{(m_b(1-y) - 2E_q)(1+z)m_b}{p_\gamma \cdot q}\Delta_{i_{26}}\right).$$

4.2 Contributions from O_8 and O_7

The contribution of the diagrams where the photon is emitted from the spectator quark lines (Fig. 5) in the B and K mesons equals

$$\begin{aligned}F^1[O_8] &= C_B C_V C_N Q_u \frac{\alpha_s}{4\pi^3}\frac{1}{m_B^2}\int dE_q dz dy \frac{E_q(m_B - 2E_q)}{(1-y)\sqrt{2(m_B - E_q)}} \\ &\times \frac{E_q(2 - y(1-z))}{m_B(1-y) - E_q(2-y)(1-z)}\phi_B(E_q)\phi_v(y).\end{aligned} \tag{27}$$

Similarly, when the photon radiates from b- and s-quark lines (Fig. 5), one obtains

$$F^2[O_8] = C_B C_V C_N Q_d \frac{\alpha_s}{4\pi^3}\frac{1}{m_B^2}\int dE_q dz dy \frac{E_q(m_B - 2E_q)}{y\sqrt{2(m_B - E_q)}}\phi_B(E_q)\phi_v(y). \tag{28}$$

The contribution associated with the operator O_7 (Fig. 3 a,b) has been calculated in [14]:

$$\begin{aligned}F[O_7] &= \frac{g_s^2 m_B}{16\pi^4} C_N C_B C_V \int dy dE_q dz \phi_V(y)\phi_B(E_q)\frac{E_q^2(m_B - 2E_q)(2 - y(1-z))}{N_b q^2\sqrt{2(m_B - E_q)}}, \\ q^2 &= \left[(1-y)m_{K^*}^2 - \frac{E_q}{m_B}\left(m_B^2(1-z) + m_{K^*}^2(1+z)\right)\right](1-y) \\ N_b &= 2E_q m_B - m_B^2(1-y) - m_{K^*}^2 y(1-y).\end{aligned} \tag{29}$$

In general, we neglect the mass of the K^* meson and of its constituents. However, when we deal with infrared divergent integrals and use the cutoff parameter Λ, we cannot neglect m_{K^*} if it is larger than Λ. Therefore we take into account the finite values of m_{K^*} and m_s when calculating the matrix elements of O_7 (Figs. 2 and 3).

4.3 Exchange diagrams

Exchange diagrams, which can contribute to the decays $B \to V\gamma$ are represented in Fig. 6 for the operators O_{1u}, O_{2u}, O_3, O_4, O_5 and O_6.
For $B \to K^*\gamma$ decay the contributions of the operators O_{1u}, O_{2u} are proportional to the small CKM factor $V_{ub}V_{us}^*$ and consequently can be neglected. Also the contributions of the operators O_3, O_4 can be neglected in the approximation where the vector meson mass is equal to zero. The contribution from the operator O_5 comes from the exchange diagrams shown in Fig. 6. The expression for corresponding form factor is the following:

$$F[O_5] = -\frac{2}{3\pi^2}\frac{C_B C_V}{m_B^2}\int E_q^2 \frac{\phi_B(E_q)\phi_V(y)}{\sqrt{2(m_B - E_q)}}\frac{(1+y)}{y(1-y)}dE_q dy. \tag{30}$$

The form factor for O_6 is given by the same formula except for an additional factor 3 coming from the trace in color space: $F[O_6] = 3F[O_5]$.

4.4 Renormalization scale dependence

It is known that NLL contributions drastically reduce the large μ dependence of inclusive decay rate for $B \to X_s\gamma$; more exactly, the μ dependence of the LL term proportional to C_7^2 is canceled by explicit logarithms, proportional to α_s. As we have here an additional μ dependence in $F^1[O_2]$ and also in C_5, C_6 in the exchange diagrams, it is necessary to check whether such a cancellation also materializes in the exclusive decays $B \to V\gamma$. The μ dependence of the contributions of the operators O_5, O_6 is due to the μ dependence of the Wilson coefficients C_5, C_6 which is determined by the renormalization group equation:

$$\frac{dC_i}{d(\log\mu)} = \frac{\alpha_s}{4\pi}\gamma_{ji}^0 C_j \tag{31}$$

An approximative solution for C_5, C_6 is

$$C_5 = \frac{\alpha_s}{4\pi}\gamma_{25}^0 \log(\mu/M_W) \qquad\qquad C_6 = \frac{\alpha_s}{4\pi}\gamma_{26}^0 \log(\mu/M_W),$$

where γ_{25}^0=-2/9, γ_{26}^0=2/3. The exchange diagrams contribute in the combination $(3C_6 + C_5)F[O_5]$. On the other hand the scale dependence originating from $F[O_2]$ is the same and opposite as seen from Eq. (17) and the color matrix identity given there.

5 Numerical results and discussion

The decay amplitude is given by the following expression:

$$\begin{aligned}\mathcal{M}(B\to K^*\gamma) &= \frac{4G_F}{\sqrt{2}}em_B\epsilon_\gamma^\mu v_t\left(i\epsilon_{\mu\nu\alpha\beta}p_\gamma^\nu\epsilon_V^\alpha p_V^\beta+(p_\gamma\epsilon_V)p_{V\mu}-(p_\gamma p_V)\epsilon_{V\mu}\right)\\ &\times \Big(C_7F^0[O_7]+C_7F^{incl}[O_7]+C_2F^{incl}[O_2]+C_8F^{incl}[O_8] \\ &+ C_2F[O_2]+C_8F[O_8]+C_7F[O_7]+(C_5+3C_6)F[O_5]\Big)\,,\end{aligned} \tag{32}$$

with $F[O_2]=F^1[O_2]+F^2[O_2]$, $F[O_8]=F^1[O_8]+F^2[O_8]$.

We begin with a discussion of the individual contributions for one special case: method 2 and $\Lambda=0.2$, $\mu=5GeV$, $f_B=160$MeV [24]. The contribution associated with the operator O_7 consists of two pieces: an "inclusive" part (Fig. 2) and an "exclusive" part (Fig. 3). The contribution of the first diagram (to the total rate) is -37%, while that of the second is -20% [1]. Similarly, the contribution of the operator O_2 is altogether 55%. 51% come from the "inclusive" diagrams (Figs. 3,4 of [8]), while the exclusive contributions amount to 5% (Fig. 4a) and -1 (Fig. 4b). The operator O_8 contributes only 2.3%, which consist of 3.8% for the "inclusive" part (Fig. 9 of [8]) and of -1.5% for the "exclusive" part (Fig. 5). The contribution of the diagrams associated with the operators O_5 and O_6 is 6.2%. The $O(\alpha_s)$ corrections to C_7 amount to -5%. The contributions of the additional factors in (10) and (12) equal -7%.

Our numerical results for the $B\to K^*\gamma$ decay rate are given in Table 1 in LL and NLL approximation (for the two methods to regularize the IR divergences). The dependence on the cutoff Λ is shown in Fig. 7, while the variation with f_B is given in Fig. 8. For $f_B=160MeV$ and Λ=0.5GeV our prediction for the branching ratio is $(5.18\pm0.5)\cdot10^{-5}$ (method 1) and $(5.16\pm0.5)\cdot10^{-5}$ (method 2) (the errors refer to the scale uncertainty). For both methods, they are in agreement with the experimental value $BR(B\to K^*\gamma)=(4.2\pm0.8\pm0.6)\times10^{-5}$ [2, 23], although it is somewhat on the high side. We note that with the simple expression for the vector meson wave function $\phi_V(y)=6y(1-y)$, the prediction for the branching is lowered by $\sim 15\%$. The NLL contributions clearly reduce the scale dependence of the LL result. For the decay rate in LL approximation, the uncertainty due to the scale dependence is 27%. On the other hand, the NLL results vary between 4% and 11% for method 1 and between 4% and 21% for method 2 for $1GeV>\Lambda>0.2GeV$. This remaining scale dependence is larger than the one of the inclusive decay. However, the standard model yields indeed an 'unnaturally' low scale dependence for $b\to s\gamma$ [25]. Therefore the variation with the scale seems reasonable to us.

The uncertainty due to the unknown value of Λ is between 6% and 14% for method 1 and between 10% and 26% for method 2. The results for the two methods for $\mu=5GeV$ and $0.2GeV<\Lambda<1GeV$ differ no more than 14%. Thus in method 1, the theoretical uncertainty is quite small, in the vicinity of 20%. If this is a correct assessment, then it is clearly desirable to improve the experimental accuracy.

---

[1] Since we only calculate to order α_s, all corrections we calculate contribute linearly.

The rather strong Λ dependence of method 2 is clearly a shortcoming of this work. It arises mainly from the logarithmic cutoff singularity of the gluonic corrections to the operator O_7. A clear improvement would be to take into account three body Fock states (with an extra gluon) whose matrix element could remove the Λ divergence. This requires relations between two-and three-body wave-functions. In simple cases, such relations exist [26]. However, a realistic calculation is beyond the state-of-the art. Another source of Λ dependence lies in the "inclusive" contributions associated with the operators O_2 and O_8. To isolate it, one would need a two-loop calculation with a finite cutoff; this is beyond the scope of this paper. We note here only that the corrections to $F[O_2]$, $F[O_8]$ vanish as Λ goes to zero. We hope to return to these issues elsewhere. But if the three-body wave function indeed removes the low Λ singularity, then a relatively low value of Λ, say 0.5 GeV, would reproduce best the correct value of the branching ratio.

In conclusion, we have calculated the next-to-leading logarithmic corrections to the branching ratio of the exclusive $B \to K^*\gamma$ decay, using an "inclusive" method and an IR cutoff parameter Λ to remove possible infrared divergences. For $f_B = 160 MeV$ and Λ=0.5 GeV, the prediction for the branching ratio is $(5.18 \pm 0.5) \cdot 10^{-5}$ and $(5.16 \pm 0.5) \cdot 10^{-5}$ for two IR regularization methods we use. This corresponds to a 10% increase over the leading order calculation. The Λ dependence is sizeable, around 20%. We discuss possible ways to improve this uncertainty.

Acknowledgments

We thank Ch. Greub, S. Brodsky, A. Khodjamirian and R. Poghosian for discussions. This work was partially supported by INTAS under Contract INTAS-96-155 and by the Swiss Science Foundation.

APPENDIX A

In this Appendix we present the results for the matrix element of inclusive $b \to s\gamma$ decay associated with the operator O_7 when we use a cutoff (method 2). The corresponding diagrams for the wave function renormalization factors $Z_2^{(b)}$ and $Z_2^{(s)}$ and the vertex operator are shown in Fig. 2. Following [8], we introduce the renormalization scale in the form $\mu^2 \exp(\gamma_E)/(4\pi)$. Then the $\overline{MS}$ subtraction corresponds to subtracting poles in ϵ in the dimensional regularization scheme.

First we present the results for nonzero gluon mass and without cutoff. For that case $Z_2^{(b)}$ is given by:

$$\Sigma^{(b)} = \frac{1}{i}\frac{\alpha_s}{3\pi^3}(2\pi)^{2\epsilon}\left(\frac{\mu^2}{4\pi}\right)^{\epsilon}\exp(\epsilon\gamma_E)\int_{-\infty}^{\infty} d^d q \int_0^1 dx \frac{4m_b - 2(\hat{p'} - \hat{q})}{(q^2 - 2xp'\cdot q - r^2)^2}$$

$$(Z_2^{(b)})^{-1} - 1 = -\frac{d\Sigma^{(b)}}{d\hat{p'}}\bigg|_{\hat{p'}=m_b}, \tag{A.1}$$

where μ_0 is the gluon mass, $r^2 = xm_b^2 + (1-x)\mu_0^2 - xp^{'2}$. Then the integral over q is performed and we obtain:

$$
\begin{aligned}
&Z_2^{(b)} = 1 + \frac{\alpha_s}{3\pi}\left(1 + \int_0^1 dx \left(-4(1-x)\log\frac{\mu^2}{\Delta_b} + 8x(1-x^2)\frac{m_b^2}{\Delta_b}\right)\right) \\
&\Delta_b = x^2 m_b^2 + (1-x)\mu_0^2
\end{aligned}
\tag{A.2}
$$

The expression for $Z_2^{(s)}$ can be obtained from (A.2) via the substitution $m_b \to m_s$. The contribution of the vertex diagram Fig 2b is given by

$$
V = \frac{2\alpha_s}{3i\pi^3}\frac{em_b}{8\pi^2}\int d^4q \int_0^1 dx_1 \int_0^{x_1} dx_2 \frac{4\hat{\epsilon}\hat{k}R(p_b\cdot p_s) - 2(\hat{\epsilon}\hat{k}R\hat{q}\hat{p}_s + \hat{p}_b\hat{q}\hat{\epsilon}\hat{k}R)}{(q^2 - 2(p\cdot q) - t^2)^3} \tag{A.3}
$$

where $p = (x_1 - x_2)p_b + (1-x_1)p_s$, $t^2 = (x_1 - x_2)(m_b^2 - p_b^2) + (1-x_1)(m_s^2 - p_s^2) + x_2\mu_0^2$. After integrating over q, V can be expressed in the following form:

$$
V =< s\gamma|O_7|b >_{tree} V_1 \tag{A.4}
$$

$$
V_1 = -\frac{2\alpha_s}{3\pi}\int_0^1 dx_1 \int_0^{x_1} dx_2 \frac{x_2(m_b^2 + m_s^2)}{x_2\mu_0^2 + (1-x_2)((x_1-x_2)m_b^2 + (1-x_1)m_s^2)}.
$$

Finally, the contribution of O_7 for the case of nonzero gluon mass is given by

$$
< s\gamma|O_7|b >_{\mu_0} =< s\gamma|O_7|b >_{tree}\left(1 + V_1 + \frac{8\alpha_s}{4\pi}\log\frac{m_b}{\mu} + \left(\sqrt{Z_2^{(b)}Z_2^{(s)}} - 1\right)\right). \tag{A.5}
$$

Now we proceed to the case when we introduce a cutoff parameter Λ. We calculate the integrals for the region $|q^2| < \Lambda^2$ and use then the previous results to obtain the integrals over the region $|q^2| > \Lambda^2$. We have the following expressions:

$$
\begin{aligned}
&\Sigma_\Lambda^{(b)} = \frac{1}{i}\frac{\alpha_s}{3\pi^3}(2\pi)^{2\epsilon}\left(\frac{\mu^2}{4\pi}\right)^{\epsilon}\exp(\epsilon\gamma_E)\int_{|q^2|<\Lambda^2} d^dq \int_0^1 dx \frac{4m_b - 2(\hat{p'} - \hat{q})}{(q^2 - 2x(p'\cdot q) - r^2)^2} \\
&\frac{1}{(Z_2^{(b)})_{|q^2|<\Lambda^2}} - 1 = -\frac{d\Sigma_\Lambda^{(b)}}{d\hat{p'}}\bigg|_{\hat{p'}=m_b},
\end{aligned}
\tag{A.6}
$$

$$
V_{|q^2|<\Lambda^2} = \frac{2\alpha_s}{3i\pi^3}\frac{em_b}{8\pi^2}\int_{|q^2|<\Lambda^2} d^4q \int_0^1 dx_1 \int_0^{x_1} dx_2 \frac{4\hat{\epsilon}\hat{k}R(p_b\cdot p_s) - 2(\hat{\epsilon}\hat{k}R\hat{q}\hat{p}_s + \hat{p}_b\hat{q}\hat{\epsilon}\hat{k}R)}{(q^2 - 2(p\cdot q) - t^2)^3} \tag{A.7}
$$

We have the following integrals:

$$
\begin{aligned}
&\Sigma_{2\Lambda}^{(b1)} = \frac{2}{3\pi^3}\int_{|q^2|<\Lambda^2} d^4q \frac{1}{(q^2 - 2x(p'\cdot q) - r^2)^2} \\
&\Sigma_{2\Lambda}^{(b2)} = \frac{2}{3\pi^3}\int_{|q^2|<\Lambda^2} d^4q \frac{q\cdot p'}{p'^2(q^2 - 2x(p'\cdot q) - r^2)^2}
\end{aligned}
\tag{A.8}
$$

$$
\begin{aligned}
V^{(1)}_{\Lambda} &= \frac{4}{3\pi^3}\int_{|q^2|<\Lambda^2} d^4q \frac{1}{(q^2-2(p\cdot q)-t^2)^3} \\
V^{(2)}_{\Lambda} &= \frac{4}{3\pi^3}\int_{|q^2|<\Lambda^2} d^4q \frac{q\cdot p}{p^2(q^2-2(p\cdot q)-t^2)^3}
\end{aligned}
\tag{A.9}
$$

The integrals over the momentum q are performed using a Wick rotation and we obtain:

$$
\begin{aligned}
\Sigma^{(b1)}_{2\Lambda} &= \frac{1}{6\pi x^2 p'^2}\Big\{\Lambda^2+r^2-\sqrt{\Lambda^4+r^4+2\Lambda^2(r^2+2x^2p'^2)}- \\
&-2x^2p'^2\left[\operatorname{arctanh}\left(1+\frac{2x^2p'^2}{r^2}\right)+\operatorname{arctanh}\left(\frac{-2x^2p'^2-r^2-\Lambda^2}{\sqrt{\Lambda^4+r^4+2\Lambda^2(r^2+2x^2p'^2)}}\right)\right]\Big\} \\
\Sigma^{(b2)}_{2\Lambda} &= -\frac{1}{12\pi x^3}\Big\{\frac{1}{p'^4}\Big(\Lambda^4+r^2(r^2-2x^2p'^2)-(\Lambda^2+r^2-2x^2p'^2)\sqrt{\Lambda^4+r^4+2\Lambda^2(r^2+2x^2p'^2)}+ \\
&+2r^2\Lambda^2\Big)+4x^4\left[\operatorname{arctanh}\left(1+\frac{2x^2p'^2}{r^2}\right)+\operatorname{arctanh}\left(\frac{-2x^2p'^2-r^2-\Lambda^2}{\sqrt{\Lambda^4+r^4+2\Lambda^2(r^2+2x^2p'^2)}}\right)\right]\Big\} \\
V^{(1)}_{\Lambda} &= \frac{(-\Lambda^2(2p^2+t^2)-t^4)\sqrt{(\Lambda^2+t^2)^2+4p^2\Lambda^2}+t^2((\Lambda^4+t^4+\Lambda^2(4p^2+2t^2))}{3\pi p^2(p^2+t^2)((\Lambda^2+t^2)^2+4p^2\Lambda^2)} \\
V^{(2)}_{\Lambda} &= -\frac{(\Lambda^2(p^2+t^2)+t^4)\sqrt{(\Lambda^2+t^2)^2+4p^2\Lambda^2}-\Lambda^4(p^2+t^2)-t^2\Lambda^2(3p^2+2t^2)-t^6}{3\pi p^4(p^2+t^2)\sqrt{(\Lambda^2+t^2)^2+4p^2\Lambda^2}}
\end{aligned}
\tag{A.10}
$$

where we take $t^2 = x_2\mu_0^2$, $p^2 = (1-x_2)((x_1-x_2)m_b^2+(1-x_1)m_s^2)$, $r^2 = (1-x)\mu_0^2$. Then $(Z_2^{(b)})_{|q^2|<\Lambda^2}$ and $V_{|q^2|<\Lambda^2}$ are equal to $(p'' = \sqrt{p'^2})$

$$
\begin{aligned}
V_{|q^2|<\Lambda^2} &=< s\gamma|O_7|b>_{tree}\,\alpha_s\int_0^1 dx_1\int_0^{x_1} dx_2(m_b^2+m_s^2)\left(V^{(1)}_{\Lambda}-(1-x_2)V^{(2)}_{\Lambda}\right) \\
(Z_2^{(b)})_{|q^2|<\Lambda^2} &= 1+\alpha_s\int_0^1 dx\left(\frac{d}{d\hat{p'}}\left((4m_b-2\hat{p'})\Sigma^{(b1)}_{2\Lambda}+2\hat{p'}\Sigma^{(b2)}_{2\Lambda}\right)\right)_{\hat{p'}=m_b} = \\
&= 1+\alpha_s\int_0^1 dx\left(2m_b\frac{d}{dp''}\Sigma^{(b1)}_{2\Lambda}-2\Sigma^{(b1)}_{2\Lambda}+2m_b\frac{d}{dp''}\Sigma^{(b2)}_{2\Lambda}+2\Sigma^{(b2)}_{2\Lambda}\right)
\end{aligned}
\tag{A.11}
$$

Then the expression for $(Z_2^{(b)})_{|q^2|>\Lambda^2}$ is given by the difference between $Z_2^{(b)}$ and $(Z_2^{(b)})_{|q^2|<\Lambda^2}$ while $V_{|q^2|>\Lambda^2}$ is given by the difference of V and $V_{|q^2|<\Lambda^2}$. For both cases, we can set the gluon mass equal to zero, i.e we take the limit $\mu_0 \to 0$.

References

[1] J. Hewett et al., in “The BABAR physics book”, SLAC-Report-504, October, 1998. M. Neubert, Talk given at ICHEP98, Vancouver, Canada 1998, hep-ph/9809343.

[2] R.Ammar et al. (CLEO Collaboration), Phys. Rev. Lett. 71 (1993) 674.

[3] B. Grinstein, R. Springer and M. B. Wise, Nucl. Phys. B339 (1990).

[4] A. J. Buras, M. Misiak, M. Münz and S. Pokorski, Nucl. Phys. B424 (1994) 374.

[5] K. Adel, Y. P. Yao, Phys. Rev. D49 (1994) 495.

[6] C. Greub, T. Hurth, Phys. Rev. D56 (1997) 2934.

[7] A. Ali, C. Greub, Phys. Lett. B361 (1995) 146.

[8] C. Greub, T. Hurth, D. Wyler, Phys. Rev. D54 (1996) 3350.

[9] K. Chetyrkin, M. Misiak, M. Münz, Phys.Lett.B200 (1997) 206.

[10] A. J. Buras, A Kwiatkowski and N Pott, Phys. Lett. B414 (1997) 157.

[11] M. Ciuchini, G. Degrassi, P. Gambino and G. F. Giudice, Preprint CERN-TH-97279 (hep-ph/9710335).

[12] M. S. Alam et al. (CLEO Collaboration), Phys. Rev. Lett. 74 (1995) 2885.

[13] Z. Ligeti, M. B. Wise, Preprint FERMILAB-Pub-99/142-T. CALT-68-2224, hep-ph/9905277.

[14] C. Greub, H. Simma, D. Wyler, Nucl.Phys. B434 (1995) 39.

[15] A. Ali, H. Asatrian, C. Greub, Phys. Lett. B429 (1998) 87.

[16] A. Buras, preprint TUM-HEP-316-98, hep-ph/9806471.

[17] C. Greub, D. Wyler, Phys. Lett. B295 (1992) 293.

[18] T. Altomari, Phys. Rev. D37 (1988) 677;
N. Isgur and M. Wise, Phys. Rev. D42 (1990) 2388;
D. Wyler, Nucl.Phys. (Proc. Suppl.) 7A (1989) 358;
A. Ali, T. Ohl and T. Mannel, Phys. Lett B298 (1993) 195;
C.A. Dominguez, N. Paver and Riazuddin, Phys. Lett. B214 (1988) 459;
T.M. Aliev, A.A. Ovchinnikov and V.A. Slobodeniuk;
Phys. Lett. B237 (1990) 569;
S. Narison, Phys. Lett. B327 (1994) 354;
P. Colangelo, C.A. Dominguez, G. Narduli and N. Paver, Phys. Lett B317 (1994) 354;
P. Ball, preprint hep-ph/9308244 (unpublished);
D.R. Burford et al. (UKQCD Collab.), Nucl. Phys. B447 (1995) 425.

[19] A. Ali, V. Braun, H . Simma, Z.Phys C63 (1994) 437.

[20] G. Eilam, A. Ioannissian, R. R. Mendel, Z.Phys. C71 (1996) 95.

[21] C. Caso et al., The European Physical Journal C3 (1998) 1.

[22] S J. Brodsky, Preprint SLAC-PUB-7861, Invited talk at Workshop on Future Directions in Quark Nuclear Physics, Adelaide, Australia, 9-20 March 1998, hep-ph/9806445;
S J. Brodsky, Patrick Huet, Phys. Lett. B417 (1998) 145.

[23] T. Skwarnicki, Preprint HEPSY 97-03, hep-ph/9712253.

[24] S. Aoki et. al., Nucl.Phys.B Proc.Suppl. 60A (1998) 89, hep-lat/9711043.

[25] M. Neubert, hep-ph/9809377. To be published in the proceedings ICHEP 98, Vancouver, Canada, 1998.

[26] F. Antonuccio, S.J. Brodsky and S. Dalley (CERN), Phys.Lett.B 412 (1997) 104, hep-ph/9705413.

Figure Captions

Figure 1: Leading order contribution, associated with operator O_7.

Figure 2: Order α_s corrections for the b and s quark wave function renormalization and the operator O_7.

Figure 3: Order α_s corrections to the matrix element of the operator O_7 with gluon exchange between the quark lines.

Figure 4: Order α_s corrections to the matrix element of O_2 with gluon exchange between the quark lines and photon emission from external (a) and internal (b) quark lines. The crosses indicate the possible places of photon emission.

Figure 5: Order α_s corrections for the operator O_8 with gluon exchange. The possible places of photon emission are labelled with a cross.

Figure 6: The contributions of the operators O_i, i=1,2,3,4,5,6 with quark exchange. The possible places of photon emission are labelled with a cross.

Figure 7: The branching ratio $Br(b \to K^*\gamma/10^{-5}$ as a function of $\log[1/\Lambda(GeV)]$ for the two methods discussed and f_B=160MeV.

Figure 8: The branching ratio $Br(b \to K^*\gamma/10^{-5}$ as a function of f_B for the two methods and $\Lambda = 0.2GeV$

Table 1.
The branching ratio $BR(B \to K^*\gamma)/10^{-5}$ in LL and NLL approximation for μ=2.5GeV, 5GeV, 10Gev, Λ = 1.0,0.5,0.2GeV and f_B=160MeV.

	$\mu = 2.5GeV$	$\mu = 5GeV$	$\mu = 10GeV$
$Br^{LL}(B \to K^*\gamma)/10^{-5}$	5.91	4.65	3.70
$Br^{NLL}(B \to K^*\gamma)/10^{-5}$, Method 1,$\Lambda$ =1GeV	5.35	5.59	5.48
$Br^{NLL}(B \to K^*\gamma)/10^{-5}$, Method 1, Λ =0.5GeV	4.70	5.18	5.21
$Br^{NLL}(B \to K^*\gamma)/10^{-5}$, Method 1, Λ =0.2GeV	4.55	5.09	5.16
$Br^{NLL}(B \to K^*\gamma)/10^{-5}$, Method 2, Λ =1GeV	6.21	5.97	5.74
$Br^{NLL}(B \to K^*\gamma)/10^{-5}$, Method 2 Λ =0.5GeV	4.66	5.16	5.20
$Br^{NLL}(B \to K^*\gamma)/10^{-5}$, Method 2, Λ =0.2GeV	3.46	4.40	4.69

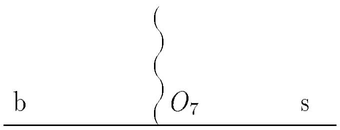

Figure 1: Leading order contribution, associated with operator O_7.

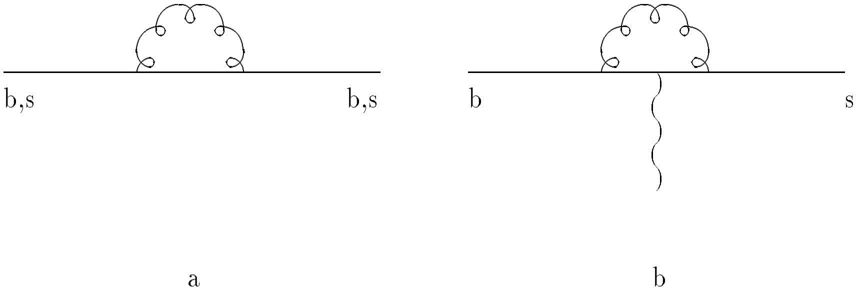

Figure 2: Order α_s corrections for the b and s quark wave function renormalization and the operator O_7.

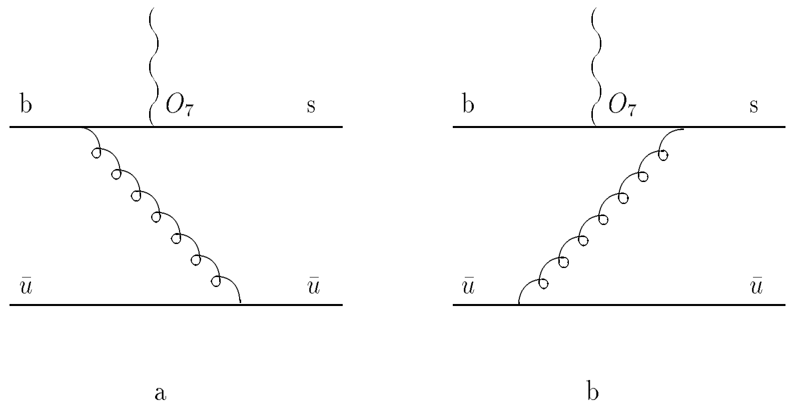

Figure 3: Order α_s corrections to the matrix element of the operator O_7 with gluon exchange between the quark lines.

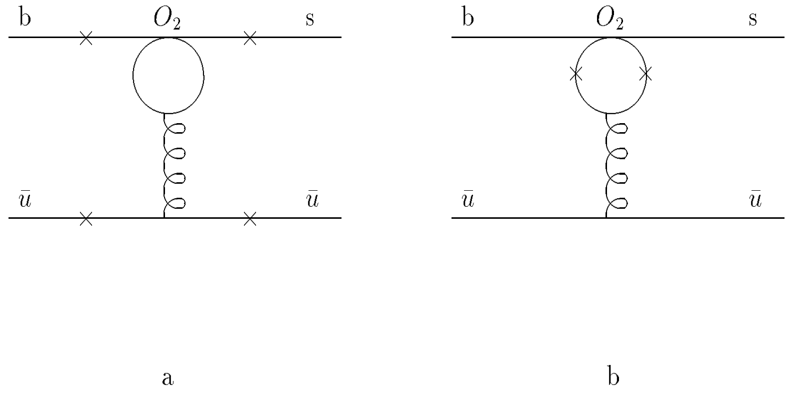

Figure 4: Order α_s corrections to the matrix element of O_2 with gluon exchange between the quark lines and photon emission from external (a) and internal (b) quark lines. The crosses indicate the possible places of photon emission.

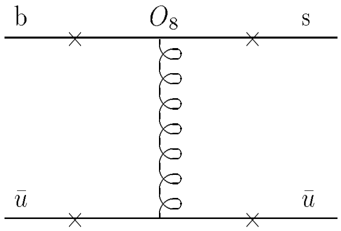

Figure 5: Order α_s corrections for the operator O_8 with gluon exchange. The possible places of photon emission are labelled with a cross.

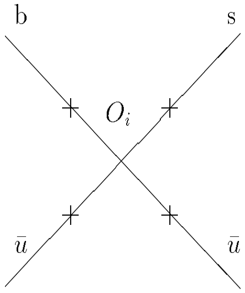

Figure 6: The contributions of the operators O_i, i=1,2,3,4,5,6 with quark exchange. The possible places of photon emission are labelled with a cross.

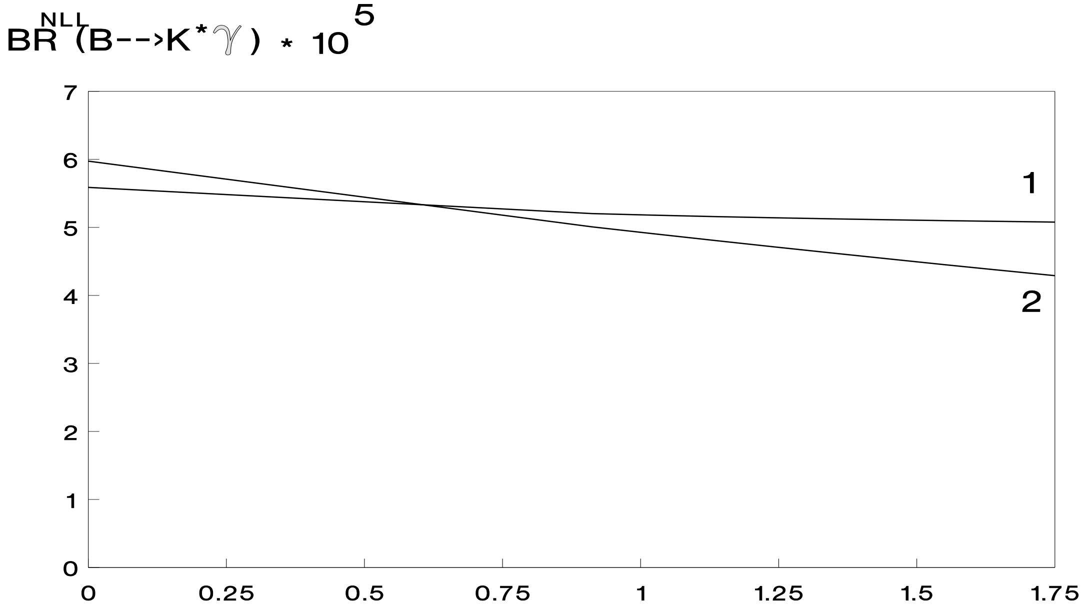

Figure 7: The branching ratio $Br(b \to K^{*}\gamma/10^{-5}$ as a function of $\log[1/\Lambda(GeV)]$ for the two methods discussed and f_B=160MeV.

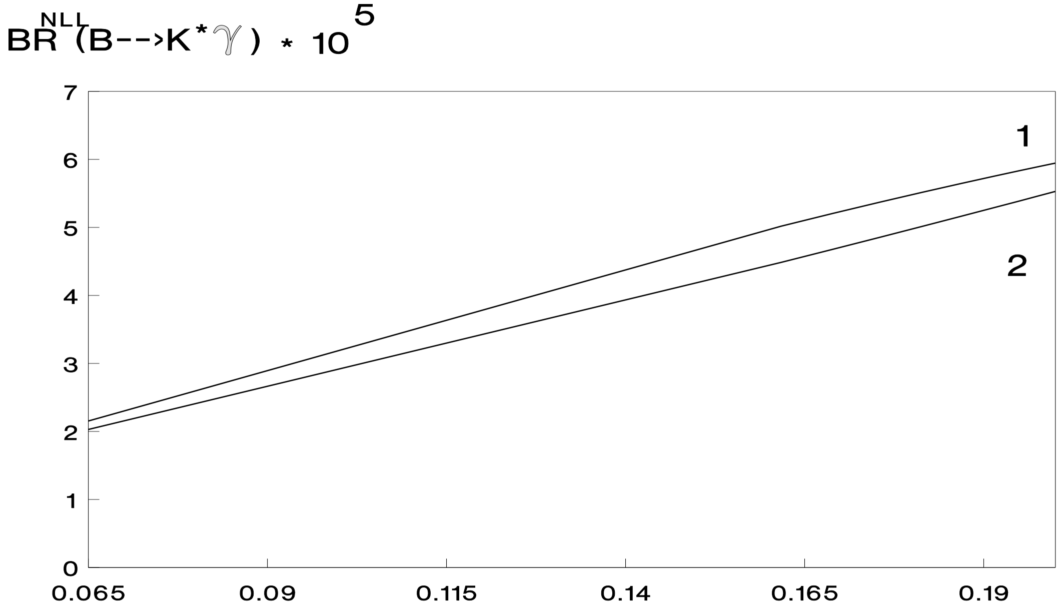

Figure 8: The branching ratio $Br(b \rightarrow K^{*}\gamma/10^{-5}$ as a function of f_B for the two methods and $\Lambda = 0.2 GeV$.